Available online at www.sciencedirect.com

ScienceDirect

Ceramics International 42 (2016) 3465–3472

CERAMICS INTERNATIONAL

www.elsevier.com/locate/ceramint

Preparation of silica-poly(2-hydroxyethyl methacrylate) hybrids modified with 3-methacryloxypropyltrimethoxysilane

Ricardo O.R. Costa[a], Fernando S. Lameiras[b], Eduardo H.M. Nunes[c], Daniela C.L. Vasconcelos[c], Wander L. Vasconcelos[c,*]

[a]*Brazilian Federal Police – Forensic Division, Rua Nascimento Gurgel, 30 – Gutierrez, CEP: 30441-170, Belo Horizonte, MG, Brazil*

[b]*Development Center of Nuclear Technology-Department of Nuclear Materials, Avenida Presidente Antônio Carlos, 6627-Campus da UFMG, CEP 31270-901, Belo Horizonte, MG, Brazil*

[c]*Department of Metallurgical and Materials Engineering, Federal University of Minas Gerais – UFMG, Avenida Presidente Antônio Carlos, 6627-Campus da UFMG, Escola de Engenharia, bloco 2, sala 2230, CEP: 31270-901, Belo Horizonte, MG, Brazil*

Received 2 September 2015; received in revised form 26 October 2015; accepted 27 October 2015
Available online 3 November 2015

Abstract

In this work we successfully prepared sol–gel derived organic–inorganic hybrids by the incorporation of poly(2-hydroxyethyl methacrylate) and 3-methacryloxypropyltrimethoxysilane into a silica matrix. The obtained samples were examined by Fourier transform infrared spectroscopy (FTIR), thermogravimetry (TG), differential scanning calorimetry (DSC), Nitrogen adsorption tests, and Vickers microhardness measurements. The incorporation of PHEMA and P(HEMA-co-MPS) into silica gave rise to samples with smaller specific surface areas and pore volumes when compared to pure silica. It was observed that materials prepared with polymer additions above 40 wt% were virtually non-porous. These findings may be related to the blockage of silica pores by polymer chains in the hybrid materials. It seems that the initial addition of either PHEMA or P(HEMA-co-MPS) to silica caused a partial filling of its pore structure, leading to an increase of its microhardness. On the other hand, when these polymers are incorporated at concentrations above 20 wt% it may occur a partial rupture of the silica framework, which decreases the microhardness of the processed materials. In addition, the increase of the polymer loading led to large polymer domains in the prepared samples. However, this behavior was less pronounced for hybrids modified with MPS.
© 2015 Elsevier Ltd and Techna Group S.r.l. All rights reserved.

Keywords: A. Sol–gel processes; B. Composites; C. Hardness; D. SiO_2

1. Introduction

Organic–inorganic hybrid materials have received great attention over the past years due to their outstanding properties, which arise from the synergy between their organic and inorganic components [1,2]. The possibility of incorporating the chemical functionality of an organic component into a thermally and mechanically reliable inorganic framework is of interest in many fields [3]. The sol–gel process stands out among the synthesis techniques generally used in the preparation of these materials. This chemical route enables to obtain hybrid materials with tailored properties, including composition, surface chemistry, and pore structure [4]. Another convenient feature of this technology is related to the fact that sol–gel samples can be obtained as bulks, thin films or powders [5].

Silica-based organic–inorganic hybrids have been widely used in a range of applications, including catalysis [6–8], membranes [9–11], water treatment [12–14], and sensing [15–17]. A variety of polymers have been used for obtaining these materials, i.e. polyetherimide [18], polyurea [19], polymethylsiloxane [20], poly(tetramethylene oxide) [21], and poly(2-hydroxyethyl methacrylate) (PHEMA) [22]. PHEMA is an attractive choice because it exhibits a significant solubility in water-alcohol mixtures commonly used in the sol–gel process. In addition, PHEMA shows a significant biocompatibility

*Corresponding author.
E-mail address: wlv@demet.ufmg.b (W.L. Vasconcelos).

http://dx.doi.org/10.1016/j.ceramint.2015.10.145
0272-8842/© 2015 Elsevier Ltd and Techna Group S.r.l. All rights reserved.

[23–25]. Although several works deal with the use of PHEMA for preparing silica-based hybrids, they rarely compare the properties of materials obtained with and without the addition of bonding agents. It is well established that the use of bonding agents may inhibit the macrophase separation in hybrid materials [26,27].

In this work we prepared sol–gel derived silica-PHEMA hybrids. 3-methacryloxypropyltrimethoxysilane (MPS) was eventually used as bonding agent, which gave rise to silica-P(HEMA-co-MPS) hybrids. The obtained samples were examined by Fourier transform infrared spectroscopy (FTIR), thermogravimetry (TG), differential scanning calorimetry (DSC), Nitrogen adsorption tests, and Vickers microhardness measurements. On the basis of the findings obtained in this study, we discuss the effect of PHEMA and P(HEMA-co-MPS) on the properties of the prepared organic–inorganic hybrids.

2. Experimental

2.1. Synthesis

PHEMA was obtained as follows. First, 2-hydroxyethyl methacrylate (HEMA – Polysciences – 99% – M_W=200,000) was dissolved at room temperature and under N_2 flow in a mixture of ethanol (EtOH – Merck – 99.8%) and 2,2′-azobis (isobutyronitrile) (AIBN – Polysciences – 98%). The concentration of HEMA in the as-prepared solution was adjusted to 20 wt%, whereas the AIBN loading was kept at 0.5 wt% of the HEMA amount. Subsequently, this solution was heated at 70 °C for 6 h. The obtained PHEMA solution was then allowed to cool down to room temperature. Silica-PHEMA hybrids were prepared by adding tetramethyl orthosilicate (TMOS – Aldrich – 98%), deionized water, and EtOH to the as-prepared PHEMA solution. The TMOS: PHEMA molar ratio ranged from 50 to 1, which gave rise to samples with PHEMA loadings from 5 to 93 wt%. The TMOS: water mass ratio was kept at 2, which corresponds to a TMOS: water molar ratio of about 0.24. After gelation the obtained solutions were aged in air at room temperature for 4 days, and at 50 and 65 °C for additional 30 and 20 h, respectively. Next, they were dried in air at 80 °C for 30 h.

PHEMA was also copolymerized with MPS (Polysciences – 99% – M_W=248) and the obtained copolymer was denoted as P(HEMA-co-MPS). This copolymer was obtained by a procedure slightly different from that used for preparing PHEMA. Briefly, HEMA and MPS were dissolved at room temperature and under N_2 flow in a solution of EtOH, AIBN, and TMOS. The MPS loading was kept at 20 wt% of the PHEMA concentration. When this methodology is compared to that used for preparing PHEMA, about 50 vol% of EtOH was replaced by TMOS. This strategy was used in order to inhibit the premature hydrolysis of MPS when in contact with EtOH. Next, the as-prepared solution was heated at 70 °C for 6 h and then allowed to cool down to room temperature. Silica-P(HEMA-co-MPS) hybrids were prepared by adding TMOS and H_2O to the as-obtained P(HEMA-co-MPS) solution. EtOH was subsequently added in amounts sufficient to promote the dissolution of the reactants. The processed samples were then aged and dried using procedure similar to that used for the silica-PHEMA hybrids. Fig. 1 depicts the methodology used for the preparation of hybrid materials in this work. SiO_2-PHEMA and SiO_2-P(HEMA-co-MPS) hybrids were denoted as SP and SPM, respectively.

A fraction of the obtained samples was subsequently heat treated at 450 °C for 1 h for further examination. This step was performed using a Lindberg Blue furnace at a heating rate of 10 °C min^{-1}. The heat treated silica, SiO_2-PHEMA, and SiO_2-P(HEMA-co-MPS) samples were denoted as HT-silica, HT-SP, and HT-SPM, respectively.

2.2. Characterization

FTIR (Fourier transform infrared spectroscopy) was performed using a PERKIN-ELMER Spectrum 1000 spectrometer. The spectra were taken from 4000 to 500 cm^{-1}, with a resolution of 4 cm^{-1} and 64 scans. Pure silica and organic–inorganic hybrid samples were examined with a diffuse reflectance attachment available in the spectrometer. PHEMA and P(HEMA-co-MPS) were tested with an attenuated total reflectance (ATR) accessory and using a zinc selenide (ZnSe) crystal as reflection element. TG (thermogravimetry) and DSC (differential scanning calorimetry) were conducted using SHIMADZU TG-50 and DSC-50 apparatus, respectively. These tests were carried out under N_2 flow (20 ml min^{-1}) at a heating rate of 10 °C min^{-1}. The glass transition temperature of the prepared samples was evaluated by DSC. N_2 sorption tests were performed in a QUANTACHROME Autosorb apparatus. Samples used in these tests were previously degassed at 110 °C for at least 12 h under vacuum. Specific surface areas and pore size distributions were assessed by the BET (Brunauer–Emmett–Teller) and BJH (Barrett–Joyner–Halenda) methods, respectively. The mean pore size (S) of the prepared samples was evaluated by assuming a cylindrical pore geometry and taking into account Eq. (1) [28]:

$$S = \frac{2PV}{SA} \quad (1)$$

where PV and SA represent the specific pore volume and surface area, respectively. Vickers microhardness tests were conducted with a FUTURE-TECH FM-1 apparatus using disk-shaped samples with 1.2 cm in diameter and 2.5 cm thick.

3. Results and discussion

Fig. 2 shows the FTIR spectra of PHEMA, P(HEMA-co-MPS), and hybrid materials prepared in this work. The spectrum of a pure silica sample is also exhibited for comparison purposes. The bands at 820 and 2840 cm^{-1} clearly observed in the spectrum of P(HEMA-co-MPS) are ascribed to Si–C and C–H bonds, respectively [28,29]. The feature at 1070 cm^{-1} has been related to the Si-O-C bending mode [30]. The bands at 1450 and 2945 cm^{-1} are associated with CH_2 groups, whereas the

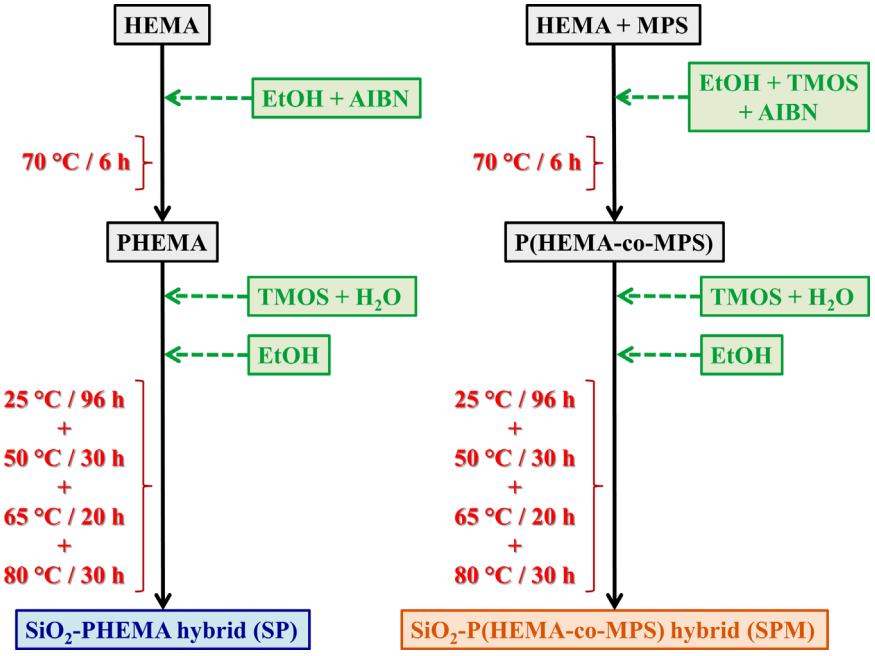

Fig. 1. Schematic representation of the steps used in this work for the preparation of samples.

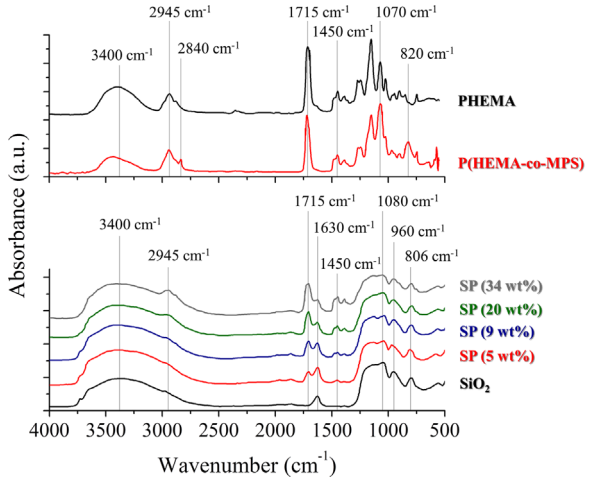

Fig. 2. FTIR spectra of PHEMA, P(HEMA-co-MPS), and hybrid materials prepared in this work. The values in parentheses represent the polymer concentration in the examined sample.

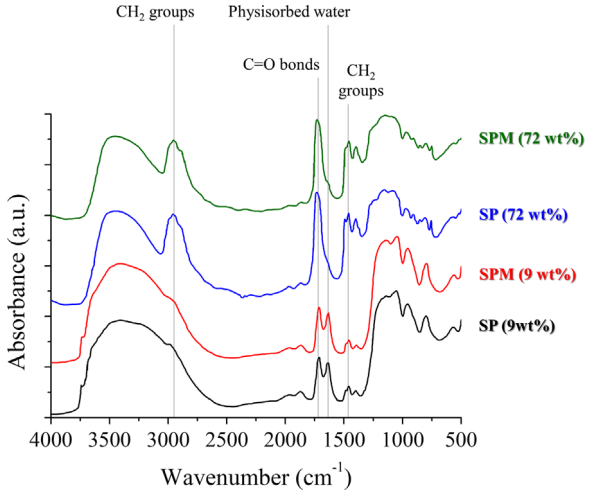

Fig. 3. FTIR spectra of SP and SPM. The values in parentheses represent the polymer loading in the examined sample.

prominent feature at 1715 cm^{-1} is ascribed to C=O bonds present in PHEMA and P(HEMA-co-MPS) [31–33]. The features at 806 and 1080 cm^{-1} observed in the spectra of pure silica and hybrid materials are related, respectively, to the asymmetric and symmetric stretching modes of Si–O bonds [34,35]. The features at 960 and 1630 cm^{-1} are ascribed to Si–OH groups and physisorbed water [36]. The broad band centered at about 3400 cm^{-1} is attributed to OH groups [37]. From Fig. 3, it can be observed that the higher the concentration of either PHEMA or P(HEMA-co-MPS), the more pronounced are the bands related to CH_2 groups and C=O bonds. In addition, the increase of this concentration decreased the feature ascribed to physisorbed water. One also notices that no significant differences are observed between the spectra of materials obtained using similar concentrations of either PHEMA or P(HEMA-co-MPS).

Fig. 4 depicts the thermograms of PHEMA, P(HEMA-co-MPS), and hybrids obtained in this study. The mass loss at temperatures up to 200 °C has been ascribed to the removal of HEMA oligomers and physisorbed water [38]. The thermal event from about 200 to 450 °C is related to the polymer degradation and elimination of non-hydrolized CH_3 groups [39]. It can be observed that P(HEMA-co-MPS) started to decompose at temperatures lower than PHEMA. Hybrid materials obtained using either PHEMA or P(HEMA-co-MPS) at concentrations up to 34 wt% exhibited TG profiles of similar shape. Nonetheless, they showed different behaviors when polymer concentrations as high as 84 wt% were used in their preparation. It was also observed that the higher the polymer concentration, the more pronounced is the mass loss assessed in the TG tests.

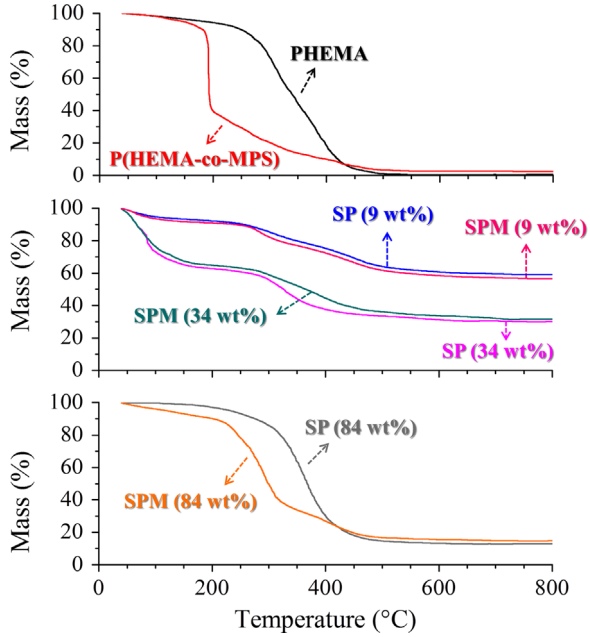

Fig. 4. TG profiles of PHEMA, P(HEMA-co-MPS), and hybrid materials obtained in this study.

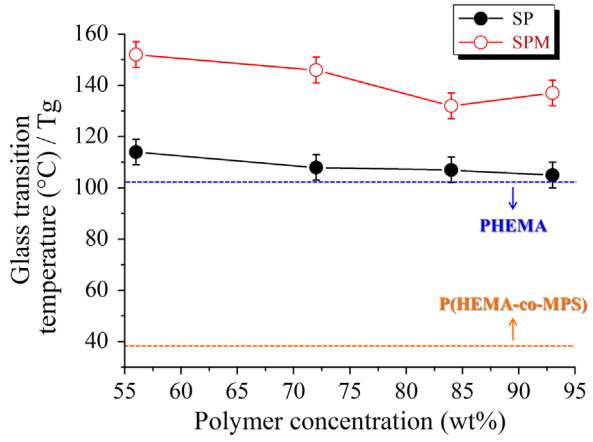

Fig. 5. Glass transition temperature (T_g) as a function of the polymer concentration for hybrids obtained in this work. The values assessed for PHEMA and P(HEMA-co-MPS) are also shown for reference purposes. T_g was obtained on the basis of DSC tests.

Fig. 5 exhibits the glass transition temperature (T_g) as a function of the polymer concentration for hybrids obtained in this study. The values assessed for PHEMA and P(HEMA-co-MPS) are also shown for reference purposes. It can be noticed that P(HEMA-co-MPS) showed a T_g significantly lower than PHEMA. This behavior is associated with the existence of Si $(OCH_3)_3$ groups in the copolymer; it is well established that they increase the spacing between adjacent polymer chains and inhibit the formation of interchain hydrogen bonds [40]. This scenario increases the mobility of the polymer chains and leads to the decrease of T_g [41]. According to Hajji et al. [42], the pendant hydroxyl groups of PHEMA favor the presence of hydrogen bonds between adjacent polymer chains.

We noticed that the incorporation of either PHEMA or P (HEMA-co-MPS) into the silica framework gave rise to hybrids with T_gs (glass transition temperatures) higher than the polymers used in their preparation. This behavior is related to the inhibition of the mobility of polymer chains by the silica matrix, leading to the increase of T_g [43]. The significant difference observed for the T_gs of SP and SPM is associated with the distinct methodologies used for preparing these materials, which could lead to the macrophase separation in these systems. It has been reported that this segregation can be controlled by changing the synthesis conditions [26,27,38].

Fig. 6 displays the N_2 adsorption isotherms of pure silica, SP, and SPM, whereas Fig. 7 shows their specific surface area and mean pore size. It was noticed that the hysteresis loop ascribed to the capillary condensation of N_2 in mesopores was more pronounced in hybrid materials than in pure silica. In addition, this hysteresis loop was more prominent for SP when compared to SPM, and became wider when the polymer loading was increased. An open hysteresis loop was observed for hybrids obtained using polymer loadings as high as 34 wt%. This finding could be associated with the entrapment of N_2 molecules into the hybrid pores, which leads to the observed difference between the adsorption and desorption

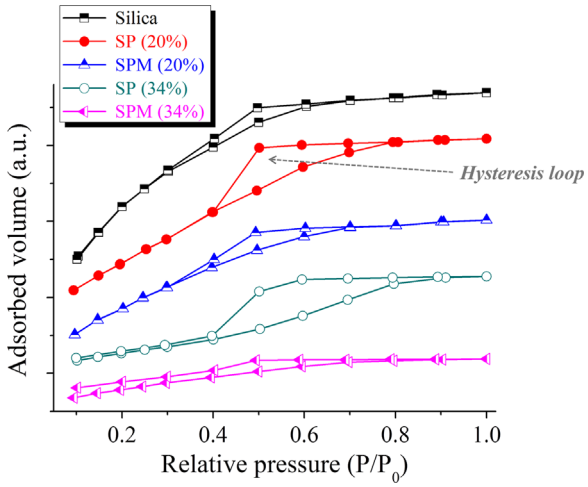

Fig. 6. N_2 adsorption isotherms of pure silica, SP, and SPM.

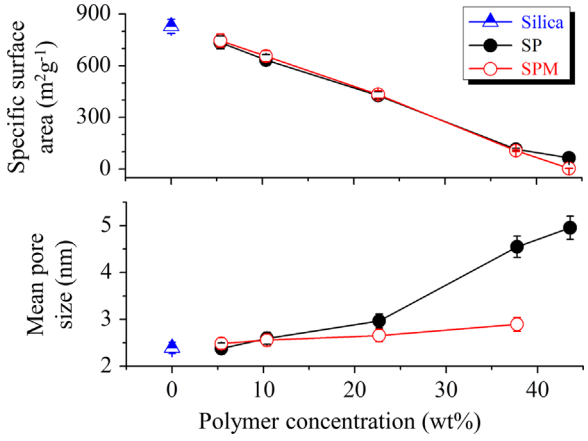

Fig. 7. Specific surface area and mean pore size of pure silica, SP, and SPM.

branches [44,45]. We observed that the increase of the polymer concentration led to materials with smaller specific surface areas. On the other hand, the mean pore size of the prepared samples increased with increasing the concentration of PHEMA or P(HEMA-co-MPS). This behavior is related to the blockage of pores in the silica network by these polymers. It was observed that hybrids with polymer additions above 40 wt% are virtually non-porous. Fig. 8 exhibits the pore size distribution of silica, SP, and SPM. We observed that silica showed a significant presence of pores with sizes about 2 nm. However, this behavior was not noticed for SP and SPM. Again, this observation is associated with the blockage of silica pores by polymer chains.

It is well established that in the sol–gel process the hydrolysis and condensation of alkoxides give rise to a colloidal suspension where nanoparticles are dispersed in a liquid medium. These primary particles subsequently agglomerate and cross-link each other, leading to a three-dimensional inorganic network enclosed by a continuous liquid phase [46,47]. For organic–inorganic hybrid systems such as those prepared in this work, polymer chains and solvent molecules are present in this liquid phase. The solvent molecules can be removed from the material upon a post-synthesis treatment. When the polymer concentration is increased, large polymer domains may be formed in the system, which could lead in turn to the segregation of phases. Moreover, in case the polymer and solvent show a noticeable compatibility, large pores may be observed in the prepared sample when the solvent is removed from the silica matrix. Because of this behavior the hysteresis loop observed in the N_2 adsorption isotherms became wider and the mean pore size of the obtained materials increased when the polymer concentration was also increased (Figs. 6 and 7). The wider hysteresis loop observed for SP when compared to SPM suggests the existence of larger polymer domains in the former. This hypothesis is also supported by the larger mean pore size exhibited by materials obtained using PHEMA instead of P(HEMA-co-MPS). As already discussed, the use of bonding agents such as that employed in this study (MPS) may inhibit the macrophase separation in hybrid materials.

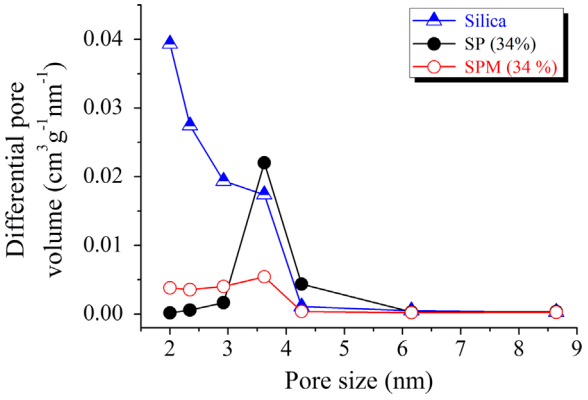

Fig. 8. Pore size distribution of silica, SP, and SPM. SP and SPM were prepared using a 34 wt% polymer loading.

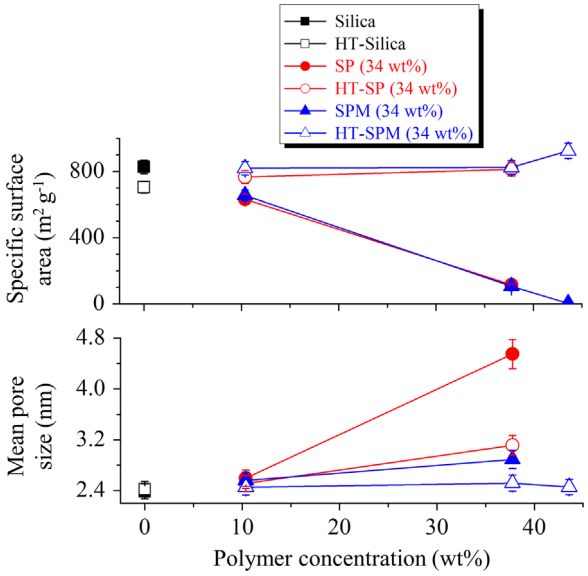

Fig. 9. Specific surface area and mean pore size of as-prepared and heat-treated samples. Solid and open symbols are associated with samples in the as-prepared and heat treated conditions, respectively.

Fig. 9 depicts the specific surface area and mean pore size of samples heat treated at 450 °C for 1 h. The values obtained for as-prepared samples are also shown for comparison purposes. We observed that the heat treatment of polymer-containing materials led to samples with larger surface areas and smaller pore sizes. This behavior is related to the removal of polymer chains from silica pores during the calcination step. One notices that this scenario is more pronounced the higher the polymer loading, which is ascribed to the formation of the aforementioned polymer domains. It was also observed that silica showed a slight decrease of its surface area when heat treated at 450 °C. This finding may be ascribed to a partial closure of the silica pore structure upon calcination. Fig. 10 exhibits the N_2 adsorption isotherms of as-prepared and heat-treated materials. On one hand, the hysteresis loop showed a slight decrease when silica was calcined. On the other hand, it became wider when heat-treated hybrids are compared to the as-prepared ones. Fig. 11 depicts the pore distribution of HT-silica, HT-SP, and HT-SPM. It can be observed that HT-SP and HT-SPM showed a higher concentration of pores with sizes about 3.5 nm when compared to the as-prepared samples. Again, this behavior is associated with the removal of polymer chains from the silica pore structure during the heat treatment step.

Fig. 12 shows the Vickers microhardness as a function of the polymer concentration for materials obtained in this study. It can be observed that an initial increase of the polymer loading from 0 to 20 wt% increased the hybrids microhardness, but further additions caused a sharp decrease of this property. The initial incorporation of polymers into silica led to a partial filling of its pore structure by polymer chains, causing the observed increase of the microhardness. Nonetheless, when the polymer is added at concentrations above 20 wt% it may occur a partial rupture of silica framework, which decreases the samples microhardness. As

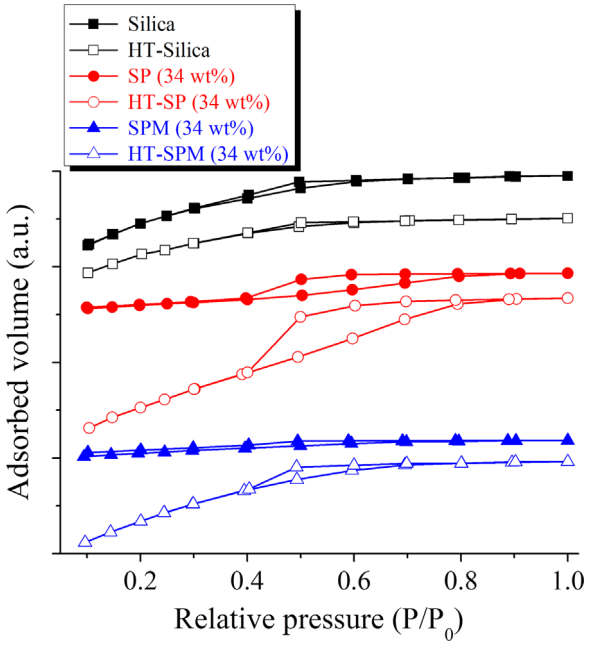

Fig. 10. N_2 adsorption isotherms of as-prepared and heat-treated samples. Hybrids prepared using a 34 wt% polymer loading. The solid and open symbols are associated with samples in the as-prepared and heat-treated conditions, respectively.

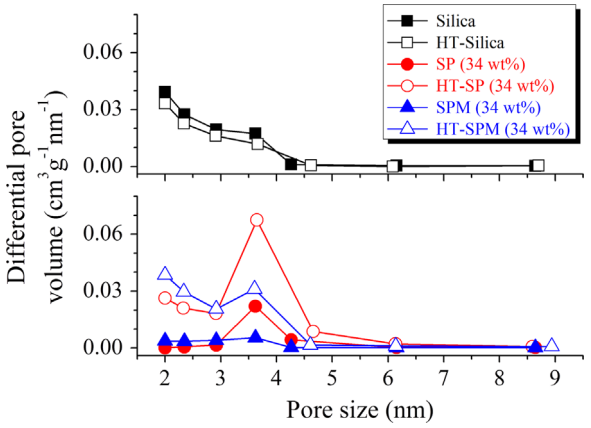

Fig. 11. Pore size distribution of HT-silica, HT-SP, and HT-SPM. Hybrids obtained with a 34 wt% polymer loading.

evidenced in Fig. 12, PHEMA show a microhardness significantly lower than silica. It is also worth highlighting the higher microhardness of SP when compared to SPM. As shown in Figs. 6–8, SP and SPM exhibit distinct N_2 adsorption isotherms and pore size distributions, which may account for the observed difference in their microhardnesses. SEM (scanning electron microscopy) tests (not shown in this work) revealed the presence of a high concentration of cracks around the pyramidal imprint formed on the silica surface after the Vickers microhardness tests. However, a crack-free and smooth surface was formed around the imprint observed on hybrids prepared with polymer loadings below 20 wt%.

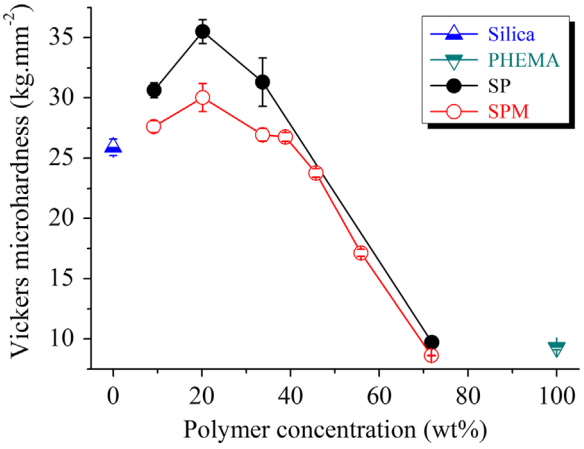

Fig. 12. Vickers microhardness as a function of the polymer concentration for SP and SPM. The values obtained for pure silica and PHEMA are also shown for reference purposes.

4. Conclusions

Absorption bands ascribed to PHEMA and P(HEMA-co-MPS) were clearly observed in the FTIR spectra of the hybrids obtained in this work. The increase of the concentration of these polymers led to both an increase of the bands ascribed to CH_2 groups and C=O bonds, and a decrease of the features related to physisorbed water. Hybrid samples showed a T_g larger than the polymers used in their preparation. This behavior is associated with the inhibition of the mobility of polymer chains by the silica matrix. The incorporation of PHEMA and P(HEMA-co-MPS) into the silica framework gave rise to samples with smaller specific surface areas and pore volumes when compared to pure silica. It was observed that materials prepared with polymer additions above 40 wt% were virtually non-porous. These findings are related to the blockage of pores in the silica structure by polymer chains. The increase of the polymer loading led to large polymer domains in the prepared samples. Nonetheless, this behavior was less pronounced in hybrids modified with MPS.

Vickers microhardness tests revealed that an initial increase of the polymer concentration from 0 to 20 wt% increased the hybrids microhardness. However, further additions of either PHEMA or P(HEMA-co-MPS) caused a sharp decrease of this property. It appears that the initial addition of these polymers to silica caused a partial filling of its pore structure, which increases its microhardness. On the other hand, when polymers are incorporated at concentrations above 20 wt% it may occur a partial rupture of the silica framework, decreasing the microhardness of the processed materials. The findings described in this work point out that the properties of the prepared organic–inorganic hybrids are strongly related to the polymer loading in the silica matrix.

Acknowledgments

The authors thank the financial support from CNPq (46.8181/00-8), FAPEMIG (CEX 554/03), and CAPES (PROEX 433/2010).

References

[1] C. Sanchez, B. Lebeau, F. Chaput, J.-P. Boilot, Optical properties of functional hybrid organic–inorganic nanocomposites, Adv. Mater. 15 (2003) 1959–2036.

[2] G. Kickelbick, Concepts for the incorporation of inorganic building blocks into organic polymers on a nanoscale, Prog. Polym. Sci. 28 (2003) 83–114.

[3] G. Kickelbick, Hybrid materials – past, present and future, Hybrid Mater. 1 (2014) 39–51.

[4] L.L. Hench, W.L. Vasconcelos, Gel-silica science, Annu. Rev. Mater. Sci. 20 (1990) 269–298.

[5] A. Yasumori, H. Shinoda, Y. Kameshima, S. Hayashi, K. Okada, Photocatalytic and photoelectrochemical properties of TiO_2-based multiple layer thin film prepared by sol–gel and reactive-sputtering methods, J. Mater. Chem. 11 (2001) 1253–1257.

[6] R.K. Sharma, S. Gulati, A. Pandey, A. Adholeya, Novel, efficient and recyclable silica based organic–inorganic hybrid Nickel catalyst for degradation of dye pollutants in a newly designed chemical reactor, Appl. Catal. B 125 (2012) 247–258.

[7] R.K. Sharma, Y. Monga, A. Puri, G. Gaba, Magnetite (Fe_3O_4) silica based organic–inorganic hybrid copper (ii) nanocatalyst: a platform for aerobic N-alkylation of amines, Green Chem. 15 (2013) 2800–2809.

[8] R.K. Sharma, S. Sharma, S. Dutta, R. Zboril, M.B. Gawande, Silica-nanosphere-based organic–inorganic hybrid nanomaterials: synthesis, functionalization and applications in catalysis, Green Chem. 1 (2015) 1–24.

[9] A.C. Ibrahim, M. Meyer, S. Devautour-Vinot, J.-P. Habas, S. Clément, D. Naoufal, A. Mehdi, A facile synthesis of proton-conducting organic–inorganic membranes, J. Membr. Sci. 470 (2014) 189–196.

[10] S. Suzuki, S.B. Messaoud, A. Takagaki, T. Sugawara, R. Kikuchia, S. T. Oyama, Development of inorganic–organic hybrid membranes for carbon dioxide/methane separation, J. Membr. Sci. 471 (2014) 402–411.

[11] M. ten Hove, A. Nijmeijer, L. Winnubst, Facile synthesis of zirconia doped hybrid organic inorganic silica membranes, Sep. Purif. Technol. 147 (2015) 372–378.

[12] M.V. Lombardo, M. Videla, A. Calvo, F.G. Requejo, G.J.A.A. Soler-Illia, Aminopropyl-modified mesoporous silica SBA-15 as recovery agents of Cu(II)-sulfate solutions: adsorption efficiency, functional stability and reusability aspects, J. Hazard. Mater. 223–224 (2012) 53–62.

[13] L. Xu, Y. Liu, H. Hu, Z. Wu, Q. Chen, Synthesis, characterization and application of a novel silica based adsorbent for boron removal, Desalination 294 (2012) 1–7.

[14] Y. Zhao, J. Li, S. Zhang, X. Wang, Amidoxime-functionalized magnetic mesoporous silica for selective sorption of U(VI), RSC Adv. 4 (2014) 32710–32717.

[15] R. Pardo, M. Zayat, D. Levy, Photochromic organic–inorganic hybrid materials, Chem. Soc. Rev. 40 (2011) 672–687.

[16] J. Sun, J. Ge, W. Liu, M. Lan, H. Zhang, P. Wang, Y. Wang, Z. Niu, Multi-enzyme co-embedded organic–inorganic hybrid nanoflowers: synthesis and application as a colorimetric sensor, Nanoscale 6 (2014) 255–262.

[17] J. Xu, Q. Zheng, Y. Zhu, H. Lou, Q. Xiang, Z. Cheng, Gravimetric chemical sensors based on silica-based mesoporous organic–inorganic hybrids, J. Nanosci. Nanotechnol. 14 (2014) 6551–6558.

[18] E.A. Mistri, S. Banerjee, Cross-linked sulfonated poly(ether imide)/silica organic–inorganic hybrid materials: Proton exchange membrane properties, RSC Adv. 4 (2014) 22398–22410.

[19] J.P. Moore, J.A. Shumaker, M.D. Houtz, L. Sun, A.N. Khramov, J. G. Jones, Thermal and optical properties of novel polyurea/silica organic–inorganic hybrid materials, J. Sol-Gel Sci. Technol. 63 (2012) 168–176.

[20] S. Nagappan, M.-C. Choi, G. Sung, S.S. Park, M.S. Moorthy, S.-W. Chu, W.-K. Lee, C.-S. Ha, Highly transparent, hydrophobic fluorinated polymethylsiloxane/silica organic–inorganic hybrids for anti-stain coating, Macromol. Res. 21 (2013) 669–680.

[21] J. Wen, B. Dhandapani, S.T. Oyama, G.L. Wilkes, Preparation of highly porous silica gel from poly(tetramethylene oxide)/silica hybrids, Chem. Mater. 9 (1997) 1968–1971.

[22] R.O.R. Costa, M.M. Pereira, F.S. Lameiras, W.L. Vasconcelos, Apatite formation on poly (2-hydroxyethyl methacrylate)-silica hybrids prepared by sol–gel process, J. Mater. Sci.-Mater. Med. 16 (2005) 927–932.

[23] Y. Zhang, D. Chu, M. Zheng, T. Kissel, S. Agarwal, Biocompatible and degradable poly(2-hydroxyethyl methacrylate) based polymers for biomedical applications, Polym. Chem. 3 (2012) 2752–2759.

[24] H.Y. Li, T. Führmann, Y. Zhou, P.D. Dalton, Host reaction to poly(2-hydroxyethyl methacrylate) scaffolds in a small spinal cord injury model, J. Mater. Sci.-Mater. Med. 24 (2013) 2001–2011.

[25] J. Ahn, E.-H. Sohn, S.H. Bang, J. Kang, T. Kim, H. Hong, S.-E. Kim, B.-S. Kim, J. Yoon, J.-C. Lee, Biocompatible Ag nanoparticle-embedded poly(2-hydroxyethyl methacrylate) derivative films with bacterial adhesion-resistant and antibacterial properties, Macromol. Res. 22 (2014) 337–343.

[26] W. Zhou, J.H. Dong, K.Y. Qiu, Y. Wei, Effect of 3-aminopropyltriethoxysilane on properties of poly(butyl acrylate-co-maleic anhydride)/silica hybrid materials, J. Appl. Polym. Sci. 73 (1999) 419–424.

[27] C.-K. Chan, I.-M. Chu, W. Lee, W.-K. Chin, Preparation and properties of organic–inorganic hybrid materials based on poly{(butyl methacrylate)-co- [(3-methacryloxypropyl)trimethoxysilane]}, Macromol. Chem. Phys. 202 (2001) 911–916.

[28] D.S. Varma, V.K. Dhar, Studies of nylon 6/PET polymer blends: structure and some physical properties, J. Appl. Polym. Sci. 33 (1987) 1103–1124.

[29] S. Yano, K. Nakamura, M. Kodomari, N. Yamauchi, Preparation and properties of poly(vinyl acetate)/silica-gel microhybrids, J. Appl. Polym. Sci. 54 (1994) 135–267.

[30] B.A. Zasónska, N. Boiko, O. Klyuchivska, M. Trchová, E. Petrovský, R. Stoika, D. Horák, Silica-coated γ-Fe_2O_3 nanoparticles: preparation and engulfment by mammalian macrophages, J. Nanopharm. Drug Deliv. 1 (2013) 182–192.

[31] Z.H. Huang, K.Y. Qiu, The effects of interactions on the properties of acrylic polymers/silica hybrid materials prepared by the in situ sol–gel process, Polymer 38 (1997) 521–526.

[32] T.S. Perova, J.K. Vij, H. Xu, Fourier transform infrared study of poly (2-hydroxyethyl methacrylate) PHEMA, Colloid. Polym. Sci. 275 (1997) 323–332.

[33] S.H. Kim, S.-H. Kim, S. Nair, E. Moore, Reactive electrospinning of cross-linked poly(2-hydroxyethyl methacrylate) nanofibers and elastic properties of individual hydrogel nanofibers in aqueous solutions, Macromolecules 38 (2005) 3719–3723.

[34] J. Román, S. Padilla, M. Vallet-Regí, Sol–gel glasses as precursors of bioactive glass ceramics, Chem. Mater. 15 (2003) 798–806.

[35] H.Y. Jung, R.K. Gupta, E.O. Oh, Y.H. Kim, C.M. Whang, Vibrational spectroscopic studies of sol–gel derived physical and chemical bonded ORMOSILs, J. Non-Cryst. Solids 351 (2005) 372–379.

[36] B.C. Smith, Infrared spectral interpretation: a systematic approach, CRC Press, New York, 1998.

[37] R.M. Almeida, G.S. Pantano, Structural investigation of silica gel films by infrared spectroscopy, J. Appl. Phys. 68 (1990) 4225–4232.

[38] S.-L. Huang, W.-K. Chin, W.P. Yang, Viscosity, particle size distribution, and structural investigation of tetramethyloxysilane/2-hydroxyethyl methacrylate sols during the sol–gel process with acid and base catalysts, J. Polym. Sci. Polym. Phys 42 (2004) 3476–3486.

[39] L.L. Hench, S.H. Wang, The sol–gel glass transformation of silica, Phase Transit. 24–26 (1990) 785–834.

[40] R.O.R. Costa, W.L. Vasconcelos, Structural modification of poly(2-hydroxyethyl methacrylate)-silica hybrids utilizing 3-methacryloxypropyltrimethoxysilane, J. Non-Cryst. Solids 304 (2002) 84–91.

[41] S. Yano, Preparation and characterization of hydroxypropyl cellulose/silica micro-hybrids, Polymer 35 (1994) 5565–5570.
[42] P. Hajji, L. David, J.F. Gerard, J.P. Pascault, G. Vigier, Synthesis, structure, and morphology of polymer-silica hybrid nanocomposites based on hydroxyethyl methacrylate, S 37 (1999) 3172–3187J. Polym. Sci. B-Polym. Phys. 37 (1999) 3172–3187.
[43] J. Jang, H. Park, In situ sol–gel process of polystyrene/silica hybrid materials: effect of silane-coupling agents, J. Appl. Polym. Sci. 85 (2002) 2074–2083.
[44] K.S.W. Sing, D.H. Everett, R.A.W. Haul, L. Moscou, R.A. Pierotti, J. Rouquérol, T. Siemieniewska, Reporting physisorption data for gas/solid systems with special reference to the determination of surface area and porosity, Pure Appl. Chem. 57 (1985) 603–619.
[45] T.X. Nguyen, S.K. Bhatia, Kinetic restriction of simple gases in porous carbons: transition-state theory study, Langmuir 24 (2008) 146–154.
[46] G. Orcel, L.L. Hench, I. Artaki, J. Jonas, T.W. Zerda, Effect of formamide additive on the chemistry of silica sol–gels-II. Gel structure, J. Non-Cryst. Solids 105 (1988) 223–231.
[47] C.J. Brinker, C.S. Ashley, R.A. Cairncross, K.S. Chen, A.J. Hurd, S. T. Reed, J. Samuel, P.R. Schunk, R.W. Schwartz, C.S. Scotto, Sol–gel derived ceramic films: fundamentals and applications, in: K.H. Stern (Ed.), Metallurgical and Ceramic Protective Coatings, Chapman & Hall, London, 1996, pp. 112–151.